Cell Death & Differentiation (2021) 28:730–747
https://doi.org/10.1038/s41418-020-00619-5

Cell Death & Differentiation

ARTICLE

Heat stress induced arginylation of HuR promotes alternative polyadenylation of *Hsp70.3* by regulating HuR stability and RNA binding

Kamalakshi Deka[1] · Sougata Saha[1,2]

Received: 23 December 2019 / Revised: 27 August 2020 / Accepted: 1 September 2020 / Published online: 14 September 2020

Abstract

Arginylation was previously found to promote stabilization of heat shock protein 70.3 (*Hsp70.3)* mRNA and cell survival in mouse embryonic fibroblasts (MEFs) on exposure to heat stress (HS). In search of a factor responsible for these phenomena, the current study identified human antigen R (HuR) as a direct target of arginylation. HS induced arginylation of HuR affected its stability and RNA binding activity. Arginylated HuR failed to bind *Hsp70.3* 3′ UTR, allowing the recruitment of cleavage stimulating factor 64 (CstF64) in the proximal poly-A-site (PAS), generating transcripts with short 3′UTR. However, HuR from *Ate1* knock out (KO) MEFs bound to proximal PAS region with higher affinity, thus excluded CstF64 recruitment. This inhibited the alternative polyadenylation (APA) of *Hsp70.3* mRNA and generated the unstable transcripts with long 3′UTR. The inhibition of RNA binding activity of HuR was traced to arginylation-coupled phosphorylation of HuR, by check point kinase 2 (Chk2). Arginylation of HuR occurred at the residue D15 and the arginylation was needed for the phosphorylation. Accumulation of HuR also decreased cell viability upon HS. In conclusion, arginylation dependent modifications of HuR maintained its cellular homeostasis, and promoted APA of *Hsp70.3* pre-mRNA, during early HS response.

Introduction

Post-translational modification (PTM) is unequivocally one of the most important factors contributing to the complexity and functionality of the proteome. One of the less explored PTM is protein arginylation, arginyl-tRNA-protein transferase (ATE1) dependent addition of arginine (Arg). Earlier studies suggested, arginylation solely occurs at the N-terminus which require prior proteolysis or removal of methionine [1–5]. However, arginylation of acidic side-chains of Glu or Asp at the N-terminus or at internal sites are recently reported [6–9]. In many cases added arginine attracts ubiquitin ligases leading to ubiquitination-mediated degradation [1, 2, 10]. However, not all proteins undergo arginylation dependent degradation and the relationship between arginylation and degradation may be very complex [5, 11]. Arginylation is shown to affect the function and interaction of proteins suggesting diverse effects of arginylation on proteome [12, 13]. At the cellular level, arginylation is known to regulate various processes, ranging from cell survival and proliferation, to cell differentiation [14–16].

Till date many proteins are reported to be modified by ATE1 [5, 17–21]. One group of proteins which stand out are the proteins involved in cellular stress response, in both mammals and plants [3, 6, 19, 22, 23]. Stress-related proteins, like calreticulin (CRT) and 78-kDa glucose-regulated protein (GRP78), are reported to be arginylated during ER stress [18, 19, 22]. Chaperones like HSC70, HSP90α, HSP90β, chaperonin, and ribophorin are reported to be arginylated [5, 24]. Upon oxidative stress, regulator of G protein signaling 4 (RGS4), RGS5, and RGS16, undergo arginylation dependent degradation [17, 20, 25]. Besides,

Edited by A. Degterev

Supplementary information The online version of this article (https://doi.org/10.1038/s41418-020-00619-5) contains supplementary material, which is available to authorized users.

✉ Sougata Saha
sougata.saha@bt.nitdgp.ac.in

[1] Department of Molecular Biology and Biotechnology, Tezpur University, Napaam, Assam 784028, India

[2] Department of Biotechnology, National Institute of Technology, Durgapur, West Bengal 713209, India

ATE1 activity decreased progressively with cellular aging, which has an important link with stress [26].

Previously our laboratory revealed, loss of arginylation make mouse embryonic fibroblasts (MEFs) more susceptible to heat stress (HS) [27, 28]. Loss of arginylation caused mitochondrial damage during HS, leading to apoptotic cell death. The defect was traced to the failure of *Hsp70* and *Hsp40* transcript stabilization and their faster degradation in *Ate1* KO cells. Several past reports indicate, a crucial event in mammalian HS response is stabilization of inducible *Hsp70* transcripts post heat shock. This may augment HSP protein expression and boost heat shock response (HSR) [29–31]. Intriguingly, inhibition of protein synthesis stabilized the transcript in unstressed cells [32]. Thus it was implied, a HS regulated labile protein was responsible for faster degradation of *Hsp70* transcripts. However, till date the mechanism of stress induced *Hsp70* transcript stabilization, as well as identity of such regulatory protein is not known.

The current study investigated the mechanism and the target of arginylation that promotes cell survival and *Hsp70* transcript stability during HS.

Materials and methods

Experimental cell lines, culture condition, and heat-shock treatment

Wild type (WT) mouse embryonic fibroblast cells (MEFs) and *Ate1* knock-out (KO) MEF, which is a homozygous knock out generated as mentioned in the ref. [33] was a kind gift from Dr. Anna Kashina, University of Pennsylvania. *Ate1.1* recovered KO MEF cells (RKO1) was generated in the laboratory of Dr. Sougata Saha by retrovirus mediated stable transfection as described in the ref. [27]. HEK 293T cells were from ATCC (CRL-3216). All the cell lines were maintained in complete medium [90% Dulbecco's Modified Eagle Media (DMEM) (Himedia, Chennai, India; AL007A) supplemented with 10% fetal bovine serum (FBS) (Himedia, RM10409) and 1× Penicillin/Streptomycin (P/S) (Thermo Fisher Scientific, MA, USA; 152400620)]; at 37 °C in humidified incubator with 5% CO_2. MEF cells with passage numbers ranging from P13 to P18 were used for all the experiments. HEK 293T cells were used with the passage range of P31 to P34. Health of the cells were always monitored using microscope at high magnification (×40 and ×100) and always healthy cells were used for each experiment. As per experimental requirements, appropriate and equal number of cells/culture plate were seeded and plates were randomly allocated for control and test groups. For induction of stress, cells were incubated at 44 °C in a static incubator for different time periods, followed by a recovery (from the stress) period of 2–6 h (as described in the "Result" section) in a humidified 5% CO_2 incubator at 37 °C. Control cells were kept in a humidified 5% CO_2 incubator at 37 °C for entire duration of the experiments.

Antibodies

The following primary and secondary antibodies were used: Mouse Anti-N-terminal arginylation (N-term-Arg) monoclonal IgG1 antibody (SMC-264D, Stress Marq Biosciences INC.), mouse anti-HuR monoclonal IgG1 antibody (3A2) (MA1-167, Thermo Fisher Scientific), rabbit anti-γ-Actin polyclonal antibody (BB-AB0025, Biobharati), mouse antiCstF64 monoclonal IgM (Kappa light chain) antibody (sc-398862, Santacruz Biotechnology Inc.), mouse anti-6× His tag monoclonal IgG2b antibody (MA1-21315, Thermo Fisher Scientific), rat anti-ATE1 monoclonal antibody (6F11) (Kind gift from Prof. Anna Kashina, Upenn, Philadelphia, USA), rabbit anti-PARP monoclonal antibody (46D11, CST), goat antimouse kappa light chain specific polyclonal secondary antibody (HRP) (AP200P, Merck Millipore), goat antimouse IgG1 cross-adsorbed polyclonal secondary antibody (HRP) (A-10551, Thermo Fisher Scientific), goat antirabbit IgG (H + L) polyclonal secondary antibody (HRP) (G-21234, Thermo Fisher Scientific), and goat anti rat IgG (H + L) polyclonal secondary antibody (HRP) (A9037, Sigma-Aldrich).

Alternative poly-adenylation (APA) assay

For APA analysis, two sets of primers were designed: one set (*HSP70.3* F1: 5′ TCCCGGTGCTGGCTAGGAGACAGATA3′ and *HSP70.3* R1:5′ CAGGGAAGATAAAGCC CACGTGCA 3′) (Table S1), which amplified all the *HSP70.3* transcripts, and provided the information about total amount of *HSP70.3* transcripts, containing both proximal and distal PAS regions. Another set amplified the region having only distal PAS site (*HSP70.3* F2: 5′ GGTCAGGAGTTGCTGTGTATGACAGTTTC 3′ and *HSP70.3* R2: 5′ CTCACACAAGCAGATCACAATGCAA TG 3′) (Table S1), hence provided the information on amount of *HSP70.3* transcript having long 3′UTR. Semi-quantitative reverse transcriptase PCR (RT-PCR) was done and PCR products were run on same gel, to minimize the difference in band intensity due to variation is gel running. Bands were quantified using GelQuant.NET software provided by biochemlabsolutions.com (CA, USA). Data was plotted after normalizing with GAPDH transcript.

Gene expression analysis

For gene expression analysis 3×10^5 cells/35 mm cell culture dish was seeded. Following heat stress and recovery,

cells were harvested for RNA isolation using TRIzol reagent (Thermo Fisher Schientific, 15596026); cDNA was prepared using a 1st strand cDNA synthesis kit (Takara Clontech, Otsu, Japan; 6110A) following the protocol set by the manufacturer. Semi quantitative reverse transcriptase polymerase chain reaction (RT-PCR) was performed using primers as mentioned in Table S1. GAPDH was taken as internal control.

MTT assay

5×10^3 cells per well were seeded in a 96-well plate, and incubated for 24 h in humidified 5% CO_2 incubator at 37 °C. Following HS and recovery, 20 µl of 5 mg/ml MTT solution was added to each of the wells and incubated in the dark for 3.5 hours, in a 5% CO_2 incubator at 37 °C. At the end of the incubation, MTT solution along with medium was removed, and 150 µl of MTT Solvent (11% SDS, 1:1 of 0.2 M HCl: Isopropanol) was added. Finally, the, plate was kept in medium shaking for 15 min followed by taking OD at 590 nm.

Western blotting

Following protein isolation, samples were run on 10–12% acrylamide gel (as per experimental requirement), and transferred into polyvinylidene difluoride (PVDF) membrane with 0.45 µm pore size, using wet transfer method followed by blocking for 1 h in 5% nonfat milk, in Tris-buffered saline-tween 20 (TBST) buffer. Blocked membrane was washed 3× times with TBST buffer. Probing with primary antibody (ab) was done for 2 h at room temperature (RT), followed by 3× washing with TBST for 10 min each. Incubation with HRP conjugated secondary Ab was done for 1 h, followed by 3× washing with TBST for 10 min each, and further developed using Clarity western ECL substrate (Biorad, CA, USA; 1705060). γ-actin (Biobharati, Kolkata, India; BB-AB0025) was used as loading control. Images were taken with Chemidoc XRS imaging system (BioRad).

Protein stability assay (MG132 assay)

A total of 3×10^5 cells were seeded into 35 mm culture dish, and incubated in humidified 5% CO_2 incubator at 37 °C overnight, with three sets for each cell line. On reaching confluency of ~70%, one set was treated with dimethyl sulphoxide (DMSO) (vehicle control), and another set was treated with proteasome inhibitor, 20 µg/ml of MG132 (Sigma, MO, USA; M7449). They were then heat stressed for 30 min, followed by recovery of 6 h in humidified 5% CO_2 incubator at 37 °C. Control cells were kept without stress at 37 °C. After recovery, cells were harvested for protein isolation; western blot was done using anti-HuR Ab (Thermo, MA, USA; MA1-167). γ-actin Ab (Biobharati) was taken as loading control.

Protein degradation assay [Cyclohexamide (CHX) chase assay]

A total of 3×10^5 cells were seeded into 35 mm culture dish, and incubated in humidified 5% CO_2 incubator at 37 °C overnight. On reaching confluency of ~70%, cells were treated with 10 µg/ml of CHX (Sigma, MO, USA; C7698) for 8 h; subsequently, heat stressed for 20 min, and harvested for protein isolation, at different recovery time points of 1, 2, 3, and 4 h. Control cells were kept without stress at 37 °C. Western blotting was done using anti-HuR Ab (Thermo).

Cloning and stable over-expressed cell line preparation

HuR ORF was PCR amplified from cDNA, using a primer set as mentioned in Table S1. Amplified HuR ORF was cloned into a modified retroviral pMSCV vector, pMSCV PIG (Addgene plasmid, MA, USA; 21654) [34], using XhoI (NEB, MA, USA; R0146S), and EcoRI (NEB, MA, USA; R3101S) restriction sites. Lack of mutation was confirmed by sequencing with both forward and reverse primers (Fig. S5B). This construct was stably transfected in WT MEFs for preparation of HuR over-expressed cell line, using protocol mentioned in the ref. [27]. Positive cell line was prepared by selection under 20–40 µg/ml puromycin pressure. Confirmation of stable expression was done by western blot analysis, using a monoclonal HuR antibody and GFP analysis (Fig. S6). These cells were named as WT-HuR.

In vitro transcription and purification

Appropriate fragments of *Hsp70.3* 3′UTR were amplified from genomic DNA using three sets of primers; *HSP70.3* F3, *HSP70.3* R4 to amplify entire 3′UTR region; *HSP70.3* F3, HSP70.3 R3: to amplify the fragment having proximal PAS; *HSP70.3* F4, *HSP70.3* R4: to amplify the fragment having distal PAS (Table S1 and Fig. S8A, B). In each fragment, T7 promoter site in the 5′end, was incorporated by incorporating the sites in the forward primers. In vitro transcription was done using MegaScript transcription kit (Thermo, MA, USA; AM1333) at 37 °C for 6 h. Following transcription, template DNA was removed with TURBO DNase (2U) treatment for 15 min at 37 °C; RNA was recovered using phenol:chloroform extraction and isopropanol precipitation method. Purified RNA was assayed for purity by checking the OD value using Nanodrop and by running on agarose gel (Fig. S8C).

Biotinylated RNA-proteins pull down assay

In vitro transcribed and purified fragments of RNA were end labeled with desthio-biotin at 3′end, using RNA 3′ End Biotinylation Kit (Pierce, MA, USA; 20160), and further purified for the assay. Twenty microliter of total volume of streptavidin magnetic beads were used for each pull down reaction. Prior to binding, beads were washed twice with equal volume of Tris-Cl buffer of pH 7.5, and neutralized once with RNA capture buffer. RNA/streptavidin magnetic bead complexes were allowed to form at room temperature for 30–40 min, in a 30 µl reaction volume containing 20 pmol of biotinylated RNA, and 20 µl of RNA capture buffer. Following binding with RNA, beads were washed twice with Tris-Cl buffer of pH 7.5, and once with protein binding buffer (150 mM NaCl, 25 mM Tris-pH 7.4, 2 mM $MgCl_2$). Protein isolated (80–100 µg) using lysis buffer (150 mM NaCl, 25 mM Tris-pH 7.4, 2 mM $MgCl_2$ and 1% NP40), followed by HS of 20 min; recovery of 2 h was precleared by incubating with streptavidin beads for 1 h at 4 °C. Precleared protein/RNA/streptavidin bead complexes were then allowed to incubate at 4 °C for 1 h, in a 100 µl reaction mixture containing 70 µl of protein, 30 µl of 30% glycerol solution, and 3 µl of 10× lysis buffer. RNA–protein complex was then pulled down using magnetic stand, washed thrice with wash buffer (Tris-Cl, pH 7.4), and dissolved in 50 µl of 1× SDS loading dye (SLD), for further analysis. Western blotting was done using anti-HuR Ab (Thermo, MA, USA; MA1-167) and anti-CstF64 Ab (Santacruz Biotechnology, Texas, USA; sc398862).

For the chase experiment, transcript amplified using primer set *HSP70.3* F3 and *HSP70.3* R3 containing proximal PAS, was taken. Desthio-biotin labeled RNA concentration was kept as constant (20 pmol), and the concentration of unlabeled RNA fragment was increased to 0×, 1×, 2×, and 4× times to labeled RNA. Precleared proteins from HS-treated KO cells were taken to study the binding of HuR and CstF64. For pull down assay in presence of check point kinase 2 inhibitor (BML277) (Santacruz Biotechnology, Texas, USA; sc200700) [35–37], the transcript was amplified using primer set *HSP70.3* F3 and *HSP70.3* R4 having total 3′UTR fragment. WT cells were pretreated with 20 µM of BML277 and 20 µM MG132 for 6 h, followed by HS for 20 min and recovery of 2 h. Post HS and recovery, pull down assay was done and streptavidin retained fraction was probed with HuR Ab.

2-D gel electrophoresis

Cells were harvested for total protein isolation using IP Lysis Buffer (150 mM NaCl, 25 mM Tris-pH 7.4, 2 mM $MgCl_2$ and 1% NP-40), and briefly sonicated to ensure proper lysis. For D15A mutant, plasmid was transiently transfected into HEK 293T cells for 48 h, cells were harvested for protein isolation using non-denaturing lysis buffer (50 mM Tris-pH 7.5, 0.5 mM imidazole, 300 mM NaCl, 5 mM β-mercaptoethanol, 0.1 mM PMSF), and Ni-NTA pull down of exogenously expressed HuR mutant was done. In each experimental set-up, isolated protein was further precipitated using TCA-acetone precipitation method. Lysate:cold acetone:100% TCA were added in the ratio of 10:80:10 with proper mixing between each addition. The mixture was then incubated at −20 °C for 1 h, followed by centrifugation at 14,000 rpm for 15 min at 4 °C. Washing was done 3× times with 100 µl of ice-cold acetone, and the pellet was air dried to remove residual acetone from the sample. 100–120 µg of protein sample was solubilized in appropriate amount of rehydration buffer. 7 cm IPG strips of linear pH 3–10 and 7–10 (Biorad, CA, USA; 163-2000 and 163-2005), were rehydrated overnight with protein samples, in rehydration tray at 20 °C. The isoelectric focusing (IEF) was run using the default program in PROTEAN i12 IEF Cell (Biorad). Following 1st dimension separation, IPG strips were equilibrated in two equilibration steps: 10 min equilibration in reducing buffer (50 mM Tris-HCl, pH 8.8, 6 M urea, 2% SDS, 30% glycerol, 2% DTT), followed by 10 min incubation in alkylation buffer (50 mM Tris-HCl, pH 8.8, 6 M urea, 2% SDS, 30% glycerol, and 2.5% iodoacetamide). Equilibrated IPG strips were rinsed in 1× SDS-PAGE running buffer, loaded onto 10% polyacrylamide gels with 1 mm thickness, and transferred into 0.45 µm PVDF membrane. Westerns were done using anti-HuR antibody and N-term-Arg antibody (Stress Marq Biosciences, Victoria, Canada; SMC0264D). Images were taken with Chemidoc XRS imaging system (BioRad, USA). For every 2nd dimension gel, right next to the acidic side of the IPG strip, a molecular weight marker was run, which served the dual purposes of determining protein molecular weight and aligning two different blots.

Endogenous ubiquitination assay

The western blot procedure was modified to detect high molecular weight modified HuR bands. Following HS treatment of 20 min and recovery of 2 h at 37 °C, cell pellets were lysed by adding 1× sample loading dye (SLD) directly (100 µl/100 mm dish), and the sample boiled at 95 °C for 10 min. Electrophoresis was done by taking ~40–50 µg of whole cell lysate. To ensure the transfer of high-molecular-weight (HMW) proteins, low ampere of 125 mA for 2.5 h was used to transfer the proteins on PVDF membrane. Probing was done with monoclonal HuR antibody at low dilution (1:1000 in 5% BSA) for 3.5 h.

Site-directed mutagenesis

Site-directed mutagenesis was done using Q5 mutagenesis kit (NEB, MA, USA; E0554S) following the manufacturer's protocol. Mutagenic primers were designed using NEBase Changer tool, with point mutation in the forward primer for all the mutations (Table S1). Exponential amplification was done with mutagenic primers, using Q5 hot start high fidelity polymerase, and HuR-His clone (generated earlier in this study) as template. One microliter of PCR product was then taken for Kinase, Ligase, and Dpn1 (KLD) treatment, using KLD enzyme mix for 5 min, at room temperature. Following treatment, 5 µl of the reaction mix was transformed in NEB 5-alpha competent *E. coli* cells (NEB, MA, USA; C2987S). Positive colonies were selected for plasmid isolation, and mutants were confirmed by sequencing, using vector specific forward and reverse primers (Table S1 and Fig. S9).

Transient transfection and Ni-NTA pull down

For screening of mutants, clones (6 µg DNA) were transfected into HEK293T cells, using lipofectamine 3000 (Invitrogen, CA, USA; L3000008). Twenty-four hours of post-transfection, cells were split in the ratio of 1:2, and allowed to grow for another 24 h. One set of plates were treated with 10 µM MG-132 and another set was treated with vehicle control (DMSO) for 6 h. HS was given for 20 min, followed by 2 h of recovery at 37 °C, in presence of MG132. Proteins were isolated using nondenaturing lysis buffer [50 mM Tris pH 7.5, 0.5 mM Imidazole, 300 mM NaCl, 5 mM β-mercaptoethanol, and 0.1 mM PMSF], and sonicated on ice at 50% Amp for 30 s (three cycles) with a break of 5 min in between to ensure proper lysis, and centrifuged at 14,000 rpm/18,000 × *g* for 10 min. The supernatant was collected in a separate pre–cooled tube and protein concentration was checked using Bradford assay. Twenty microliter of Ni-NTA beads were taken, equilibrated with equilibration buffer (50 mM Tris pH 7.5, 0.5 mM Imidazole, 300 mM NaCl, and 5 mM β-mercaptoethanol), before incubating the beads with isolated protein samples. Protein and Ni-NTA beads were allowed to incubate for 1 h at 4 °C with gentle rotation. Following incubation, samples were centrifuged for 2 min at 700 × *g*, and supernatants removed. Beads were washed thrice with wash buffer (50 mM Tris pH 7.5, 25 mM Imidazole, 500 mM NaCl, 5 mM β-mercaptoethanol, and 0.1 mM PMSF), re-suspended in appropriate amount of 1× SLD directly, and boiled at 95 °C for 10 min.

Secondary structure prediction and alignment

Secondary structures of HuR protein having RNA recognition motif 1 (RRM1) and RNA recognition motif 2 (RRM2), expanding from M1 to Q189 residues, along with truncated HuR protein structures, with or without added arginine, were predicted using i-TESSAR online software server (University of Michigan, USA); [38–40] by taking HuC (PDB Id: 1FNX) (Mouse homolog primarily neuronal) [41], as a reference structure. Predicted secondary structures of HuR (1–189 HuR), and truncated HuR with and without added arginine (15–189 HuR and R15–189 HuR), were aligned using Chimera software [42].

Statistical analysis

RT-PCR analysis and Western blots which are statistically validated are representative of at least 2–3 independent experiments. All MTT experiments were done in triplicate wells and normalized as indicated in figure legends. Experimental replicate numbers are designated as "*n*" in the figure legends of each figure. As the experiments are done with homogenous cell lines, not much variation was expected within each experimental groups in in vitro experiments and hence experimental replicate size (*n*) were restricted to 2 or 3. Data are presented as mean ± s.e.m. Unpaired student *t*-tests/one-way ANOVAs were done to calculate the *p*-values using Graph Pad Prism 5.0 (GraphPad software, La Jolla, CA, USA). All statistical tests were performed with the assumption of similar variance for all test groups. No inclusion/exclusion criteria were pre–decided in any of the experiments. To avoid any false positive statistical result, the statistical significance was defined as $p < 0.05$. (**$p < 0.05$, ***$p < 0.01$, ****$p < 0.001$.)

Results

Loss of arginylation inhibits APA of *HSP70.3* transcripts upon HS

Earlier, our laboratory showed, while induction of *Hsp70.3* gene upon HS was not affected due to loss of arginylation (Fig. S3), the stability of *Hsp70.3* transcripts were severely affected [27]. APA is known to affect the stability of many transcripts [43–47] and HS-induced APA of *Hsp70.3* produces transcripts with shorter 3′UTR [48, 49]. *Hsp70.3* is an inducible heat shock protein (HSP) having four poly A sites (PAS) in its 3′UTR (Figs. S1, S3) [27]. During HS, APA from proximal PAS2 generates *Hsp70.3* transcripts having short 3′UTR (Fig. 1a and Fig. S1A, B) [48].

Investigation of stress-induced APA of *Hsp70.3* in wild type (WT) and *Ate1* KO MEFs showed, *Hsp70.3* APA was inhibited in *Ate1* KO cells (Fig. 1b). Quantification of relative levels of long and total *Hsp70.3* transcripts showed, only a small fraction out of total *Hsp70.3* transcripts had long 3′UTR in WT cells. Whereas in *Ate1* KO cells, a major

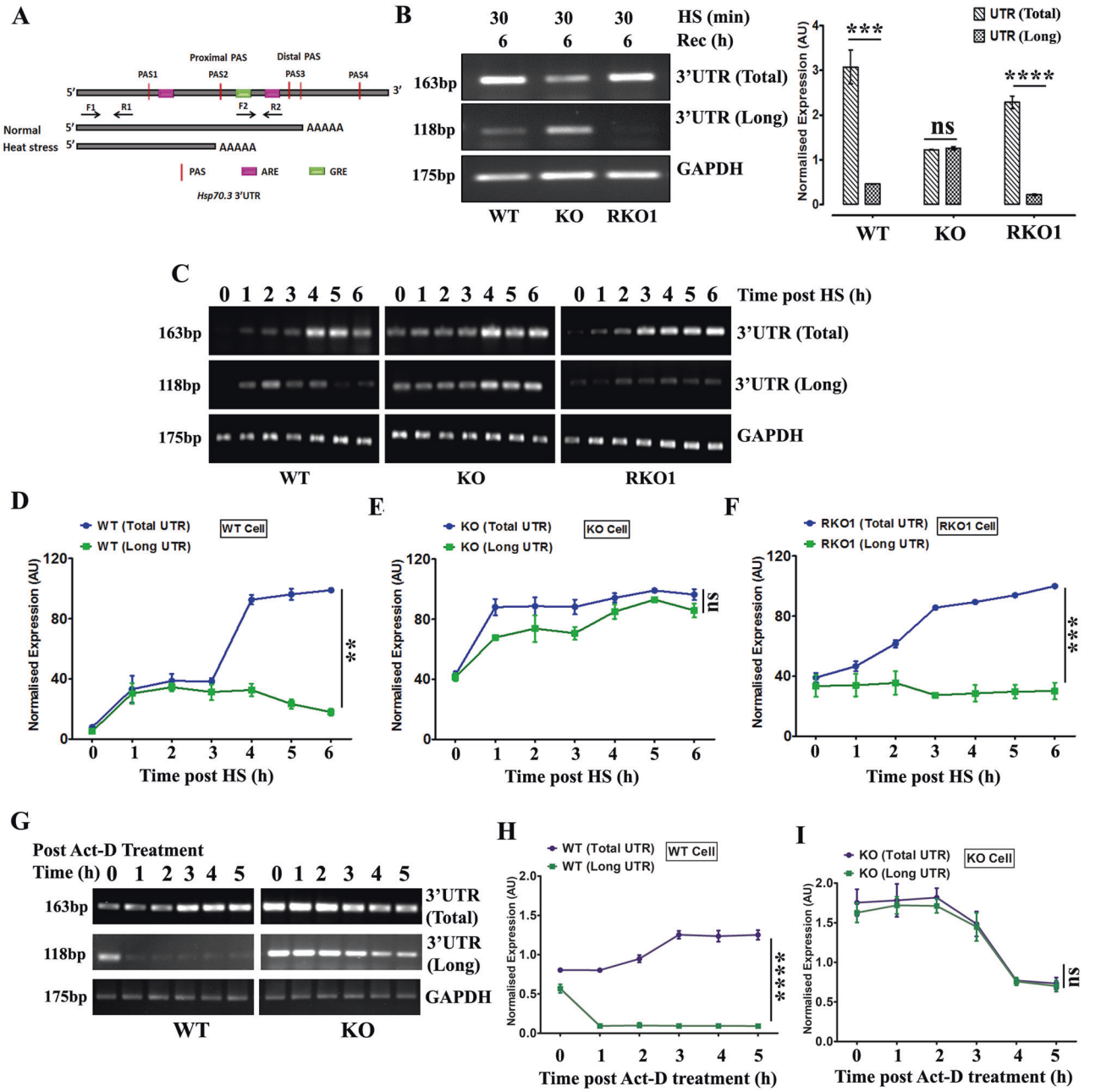

Fig. 1 Loss of arginylation inhibits alternative polyadenylation of *Hsp70.3* pre mRNA upon HS. a 3′UTR of *Hsp70.3* having four PAS with regions specified for primers designed to amplify total (F1, R1) and long 3′UTR (F2, R2). **b** Representative gel images and graph represent level of total *Hsp70.3* transcript and transcripts having long 3′UTR normalized with respect to GAPDH in WT, *Ate1* KO (KO), and RKO1 MEFs following heat shock (HS) for 30 min at 44 °C and recovery (Rec) of 6 h at 37 °C. Same temperature of HS and recovery was maintained in all the experiments. (*p* values are from unpaired *t*-test, error bar ± SEM, $n = 3$). **c–f** Panel **c** represents RT-PCR analysis for total *Hsp70.3* transcripts and transcripts having long 3′UTR in WT, *Ate1* KO (KO) and RKO1 MEFs at different time points (0–6 h) of recovery post-heat shock for 30 min. **d–f** Expression of total *Hsp70.3* transcript and transcript having long 3′UTR normalized with respect to GAPDH in WT, *Ate1* KO (KO), and RKO1 MEFs, respectively. (*p* values are from one-way ANOVA, error bar ± SEM, $n = 2$). **g–i** Panel **g** represents RT-PCR analysis for total *Hsp70.3* transcript and transcripts having long 3′UTR in WT and KO MEFs post Actinomycin-D (Act-D) (5 µg/ml) treatment. Cells were treated with Act-D post HS for 20 min and recovery of 2 h. Panels **h** and **i** represent quantification of the data after normalizing with GAPDH. (*p* values are from one-way ANOVA, error bar ±SEM, $n = 3$) $^{**}p < 0.05$, $^{***}p < 0.005$, $^{****}p < 0.0005$, ns nonsignificant.

fraction of *Hsp70.3* transcripts carried long 3′UTR (Fig. 1b). Similarly, when the ratios of long/total *Hsp70.3* transcripts were compared, a major fraction of HSP70.3 transcripts in KO cells were found with long 3′UTR (Fig. S2). The defect was reverted in *Ate1* KO cells stably expressing ATE1 isoform-ATE1-1 (recovered KO cells:

RKO1). While *Hsp70.3* transcript level increased post HS in WT cells, the long transcripts decreased during the same period (Fig. 1c, d). Conversely, the expression level of long transcripts increased steadily in KO cells post-HS (Fig. 1c, e). In RKO1 cells, the level of long transcripts remained very low at all the times (Fig. 1c, f).

To understand the relation of *Hsp70.3* transcript stability with 3′ UTR length, the stability of long transcripts was compared with the total *Hsp70.3* transcript population. It was earlier confirmed that the total population of *hsp70.3* transcripts remain stable in WT cells post-HS, while the same degrades steadily in *Ate1* KO cells [27]. Actinomycin-D (Act-D) chase experiment in the current study showed, long 3′UTR containing *Hsp70.3* transcript underwent steady degradation in both WT and KO cells (Fig. 1g–i). Thus, arginylation promoted APA of *Hsp70.3* pre-mRNA upon HS and APA mediated shortening of 3′UTR might be regulating its stability following HS.

Arginylation promotes degradation of RNA binding protein HuR and enhances cell survival upon HS

Theodorakis and Morimoto [32] showed a labile protein-regulated *Hsp70.3* transcript stability. HuR, an important regulator of mRNA stability, was recently shown to undergo proteasome mediated degradation upon HS [50]. Intriguingly HuR autoregulates its expression by promoting its APA [51]. Consequently, HuR appeared to be a critical target in arginylation dependent regulation of *Hsp70.3* transcript stability. No change was observed in the transcript level of HuR in WT, KO, and RKO1 cells, even after 60 min of HS (Fig. 2a). However, HuR protein level was altered in all the three cell lines after 30 min of HS. While HuR protein level decreased in WT and RKO1 cells, it increased in KO cells (Fig. 2b). Cycloheximide (CHX) chase assay displayed a fairly labile HuR protein post HS in WT and RKO1 cells, whereas it remained stable in KO cells (Fig. 2c). ATE1 dependent degradation of HuR was further confirmed by treating cells with MG132 (20 μM), an inhibitor of proteasome along with few other cellular proteases. In agreement with the earlier report that MG132 inhibits degradation of HuR [50], MG132 enhanced the HuR protein level in WT and RKO1 cells, compared to control cells (HS + DMSO) (Fig. 2d). Since no concomitant increase was observed in KO cells, it implied HuR underwent HS induced degradation in presence of arginylation. Contrary to previous observations, MG132 treated heat stressed WT and RKO1 cells showed severely less spread morphology and reduced viability, akin to KO cells (Fig. 2e and Fig. S4A, B). It is probable that the accumulation of single or multiple labile proteins including HuR are responsible for observed cell morphology and reduced viability.

To test the idea, mouse HuR was stably overexpressed in WT-MEF (Figs. 2f, S5A, B, and S6). The line was named WT-HuR. Overexpression of HuR protein in WT-MEF showed a decrease in cell viability upon HS (even in the absence of MG132) comparable to KO and MG132-treated cells (Fig. 2g). Cell survivability of WT cells upon HS was not affected due to transfection with empty vector (WT-VC) (Fig. S7). Thus, reduced viability of heat-stressed KO cells could be influenced by the proteostasis of HuR.

Arginylation regulates the differential binding of HuR and CstF64 to *Hsp70.3* transcripts

Considering the role of HuR in APA and its accumulation in heat-stressed KO cells, two questions were raised. (1) Does HuR bind to *Hsp70.3* 3′UTR and regulate its APA? (2) Does the HuR protein levels affect such regulation? To answer these questions, RNA-protein pull down assays were performed using three fragments of *Hsp70.3* 3′UTR: full length 3′UTR (F3R4), proximal 3′UTR with proximal PAS (F3R3) and distal 3′UTR with distal PAS (F4R4) (Figs. 3a and S8).

APA being an early event, the assay was performed after 2 h recovery post-HS. At this point, HuR level in WT, KO, and RKO1 cells were unchanged (Fig. 3b). In spite of the same levels of HuR protein, a stark contrast was observed in the binding of HuR to 3′ UTR (Fig. 3b–e). Only HuR from KO cells bound to 3′UTR. Moreover, HuR bound to the proximal fragment with much higher level compared to distal fragment. HuR from WT and RKO1 cells failed to bind *Hsp70.3* 3′UTR, signifying arginylation impacts both-the protein level of HuR and the RNA binding ability of HuR (Fig. 3b–e).

For the initiation of polyadenylation, cleavage stimulating factor 64 (CstF64) is vital (Fig. 3f, g). CstF64 from WT and RKO1 cells bound effectively with the proximal fragment and weakly to distal fragment (Fig. 3f, h, i). For KO cell, the situation was reverse (Fig. 3f, h, i). In a competitive chase assay sequestration of HuR from the heat-stressed KO cell extract, by interaction with increasing concentrations of unlabeled F3R3 fragment, led to increased binding of CstF64 to the proximal PAS fragment (F3R3) (Fig. 3j). The data affirmed the possibility that, HuR binding affected the biding of CstF64 to *Hsp70.3* 3′UTR which in turn affected the APA of *Hsp70.3* transcripts.

Arginylation regulates Chk2 dependent phosphorylation of HuR which affects its binding to 3′UTR of *Hsp70.3*

As differential binding of HuR onto Hsp70.3 3′UTR could be due to differential post-translational modifications

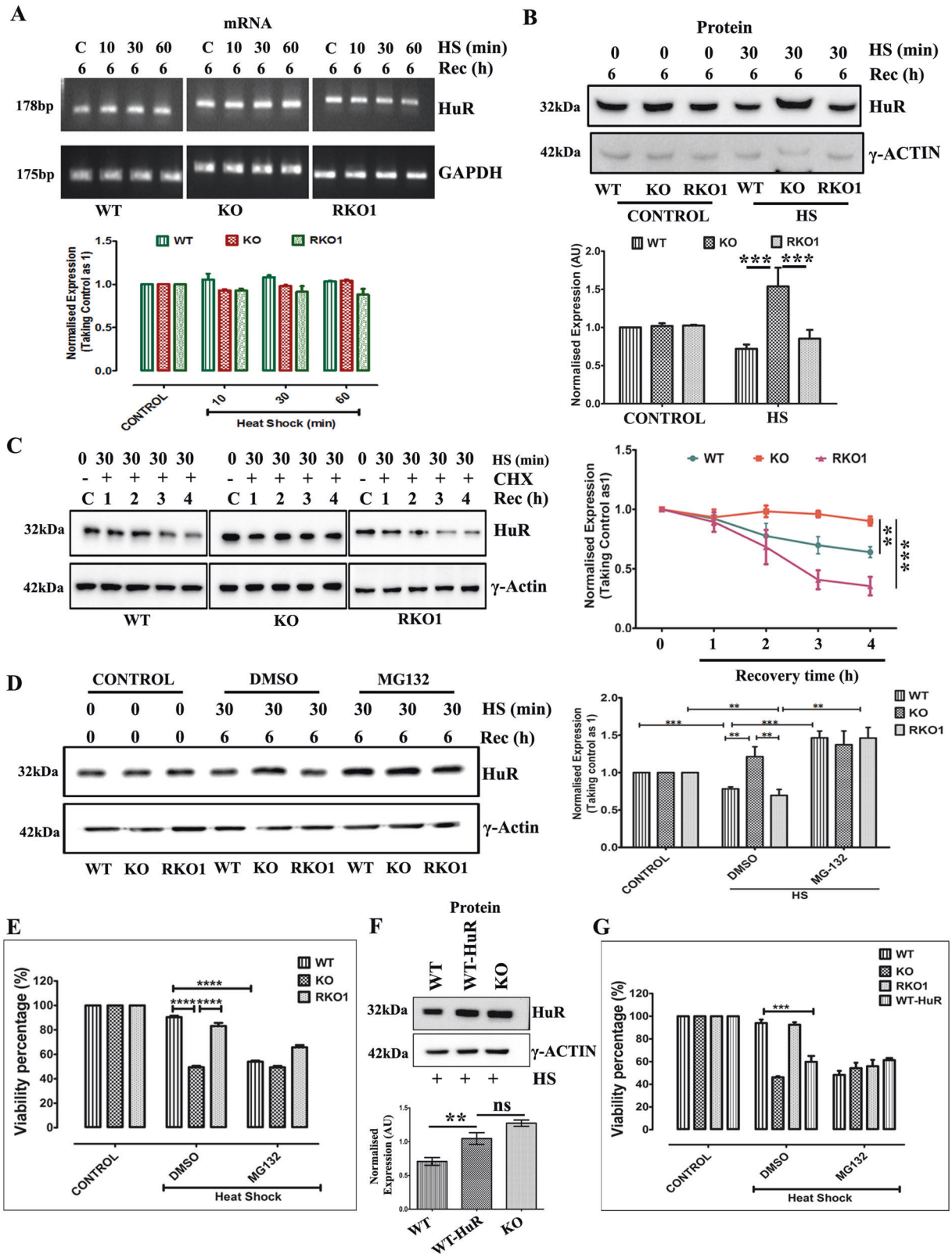

(PTM), PTM of HuR was analyzed by 2D PAGE coupled western blotting. pI of native HuR being 9.12, initial analyses were done between pH 7 and 10. Subsequent analyses were done between pH 3 and 10, using heat-stressed cells treated with MG132. These assays exhibited multiple spots of HuR protein towards the acidic side of the blots in WT

◀ **Fig. 2 Arginylation promotes proteasomal degradation of HuR and enhances cell survival upon HS. a** Representative gel images and graph represent the normalized expression of HuR mRNA in WT, KO, and RKO1 MEFs following HS for different durations followed by recovery of 6 h. Expression was normalized w.r.t GAPDH and control of each cell line. (p values are from unpaired t-test, error bar ± SEM, $n = 2$). **b** Representative gel images and graph represent normalized expression of HuR protein in control and heat stressed WT, KO, and RKO1 MEFs post-HS for 30 min and recovery for 6 h. Expression was normalized w.r.t γ-Actin and control of each cell line. (p values are from unpaired t-test, error bar ± SEM, $n = 3$) **c** Representative gel images and graph represent normalized level of HuR protein in WT, KO, and RKO1 MEFs at different durations of recovery in presence of cycloheximide (CHX) post-HS for 30 min. Level of HuR was normalized with respect to γ-Actin and control of each cell line. (p values are from one-way ANOVA, error bar ± SEM, $n = 3$) **d** Representative gel images and graph represent normalized level of HuR protein in WT, KO, and RKO1 MEFs following 30 min of HS and 6 h of recovery in presence of MG132. DMSO was vehicle control. Level of HuR was normalized with respect to γ-Actin and control of each cell line. (p values are from one-way ANOVA, error bar ± SEM, $n = 3$) **e** Viability percentage of the cells represented in **d** with respect to controls. (p values are from unpaired t-test, error bar ± SEM, $n = 3$) **f** Level of HuR protein in stably transfected WT MEFs (WT-HuR) as well as WT and KO MEFs post 30 min HS and 6 h recovery. HuR levels were normalized with respect to γ-Actin. (p values are from unpaired t-test, error bar ± SEM, $n = 2$) **g** Viability percentage of WT, WT-HuR, KO, and RKO1 MEFs with respect to controls following HS and MG-132 treatment as mentioned in **d**. (p values are from unpaired t-test, error bar ± SEM, $n = 3$) $^{**}p < 0.05$, $^{***}p < 0.005$, $^{****}p < 0.0005$.

and RKO1 cell lysates. Acidic spots were greatly diminished in *Ate1* KO cell lysates (Fig. 4a, b).

Phosphorylation of HuR, an acidic modification, by checkpoint kinase 2 (Chk2) at S88 and S100 inhibits RNA binding activity of HuR [52–55]. Treatment with Chk2 inhibitor BML277 [35] along with MG132 depleted the acidic spot of HuR at pI range 3–4 in heat-stressed WT-MEFs (Fig. 4c). Hence, the depletion of acidic HuR spot in KO cells, could be due to loss of phosphorylation (Fig. 4b). In spite of similar overall patterns of spots, somewhat difference observed in the basic range of the blots in Fig. 4c and Fig. 4b could be due to difference in the protein load. Thus, ATE1 may regulate phosphorylation of HuR by Chk2 which restricts its binding to *Hsp70.3* 3′UTR upon HS. It also raised the question: whether HuR was a direct target of arginylation.

While arginylation is possible at N-terminus or at the internal residues [6–8], many of the well characterized ATE1 substrate proteins like β-actin, calreticulin, GRP78, and RGS proteins, all are arginylated at aspartic acids (D) or glutamic acids (E) or oxidized cysteine (C) residues at N-terminal region [11, 17–20]. Arginylation on N-terminally exposed D, E, and oxidized C may also cause degradation of a protein [1, 2, 10]. Mouse HuR has four D, two E, and one C close to N-terminus, which could potentially be the sites of arginylation upon exposure due to truncation or as internal sites (Fig. 4e). Calculated pI of truncated and arginylated HuR moved towards basic side, from 9.12 (native) to 9.65 (R16) (Table S2). Careful analysis of 2D PAGE data indicated a shift of the main HuR spot (at around pI of 9.2) towards further basic range in WT and RKO1 cells as predicted (compared to KO) (Fig. 4b). The amount of HuR protein at the furthest basic range (probable arginylation) was considerably higher in RKO1 cells than in WT cells. This could be due to higher level of ATE1 expression in RKO1 cells compared to WT cells, as shown in our previous communication [27]. These observations strongly advocated that, HuR may be a novel and unreported target of arginylation.

HuR acts as a direct target for ATE1 upon HS

To confirm HuR arginylation, exogenously expressed HuR-His was pulled-down from heat-stressed WT and KO cells treated with MG132. Pulled-down HuR-His, only from WT cells, reacted with N-term-Arg ab (Fig. 5a). However, anti-HuR ab detected HuR from all the transfected samples, with enhanced high molecular weight bands in MG132-treated WT cells (Fig. 5a). The high molecular weight bands could be due to its poly-ubiquitination during HS, as reported earlier by Abdelmohsen et al. [50]. Levels of unmodified HuR in presence of MG132 remained somewhat same in WT cells. This could be due to little accumulation of HuR at the early stage (2 h) of HS response. HuR, is confirmed by the results, as a novel and unreported target of arginylation.

Arginylation of HuR is stress-inducible and acts as a signal for high molecular weight modifications of HuR

To affirm HuR arginylation is a stress-inducible phenomenon, exogenously expressed HuR–His was pulled down from control and heat-stressed WT cells, and probed with N-term-Arg ab. Arginylated HuR was predominantly detected in heat-stressed cells (Fig. 5b). Intriguingly, an increasing amount of ATE1 was localized in the nucleus over time, post stress (Fig. 5c). In agreement with the previous report [56], HuR was also mostly localized in the nucleus (Fig. 5c). Thus, it can be postulated that HuR undergoes HS induced arginylation in the nucleus as an early response to HS.

N-terminal arginylation of proteins often leads to poly-ubiquitination and degradation [1, 2, 10]. HS generated very high levels of high molecular weight HuR bands (typical of poly-ubiquitination) in WT cells but not in KO cells. High molecular weight smear disappeared significantly in presence of ATE1 inhibitor (Tannic acid-TA) [57] (Sigma, MO, USA; 403040) (Fig. 5d, e). Thus, arginylated HuR may be poly-ubiquitinated and decrease in HuR protein

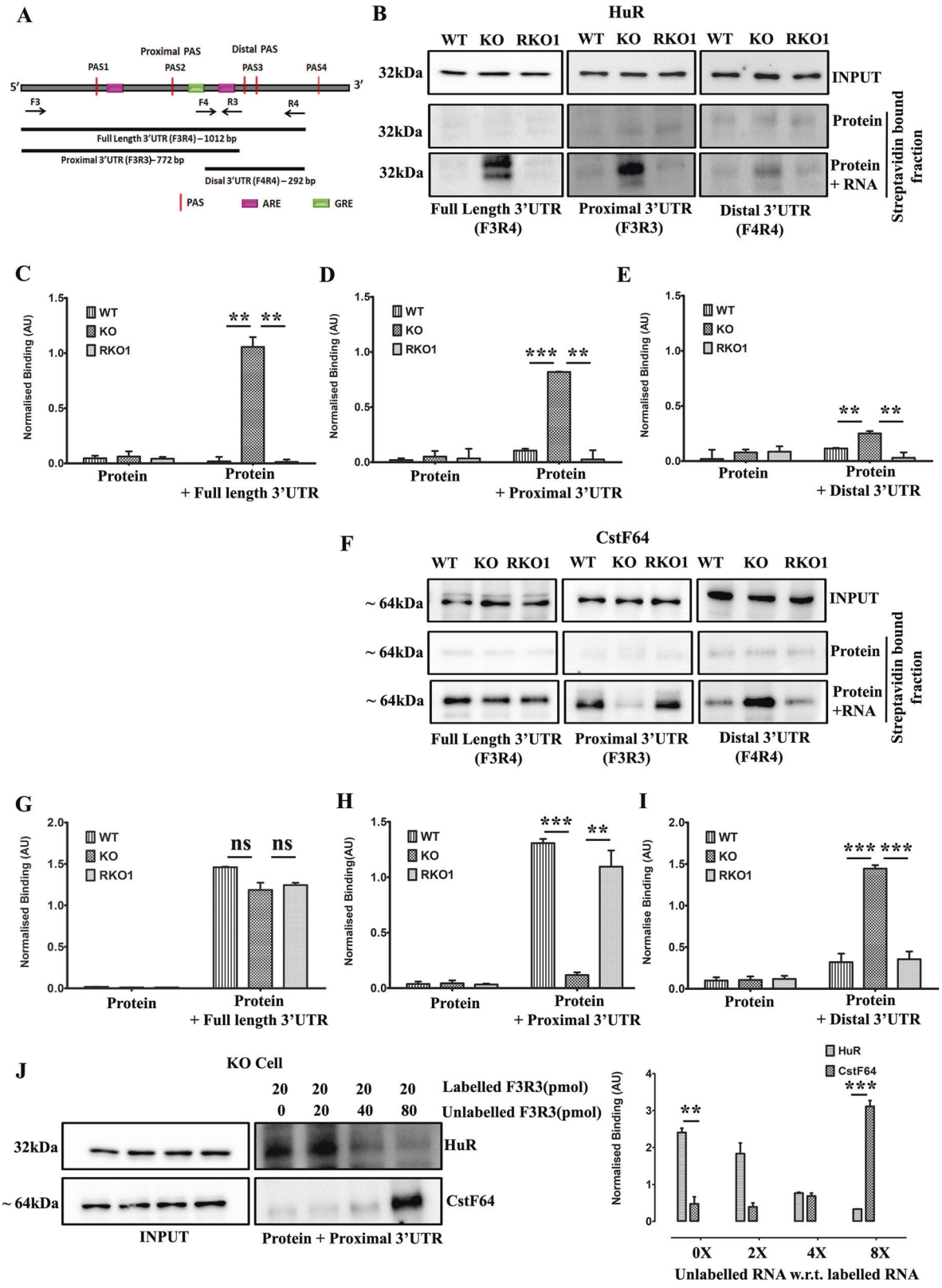
A
Proximal PAS
Distal PAS
PAS1
PAS2
PAS3
PAS4
5'
3'
F3
F4
R3
R4
Full Length 3'UTR (F3R4) – 1012 bp
Proximal 3'UTR (F3R3)– 772 bp
Disal 3'UTR (F4R4) – 292 bp
PAS
ARE
GRE
B
HuR
WT KO RKO1 WT KO RKO1 WT KO RKO1
32kDa
INPUT
Protein
Protein + RNA
Streptavidin bound fraction
Full Length 3'UTR (F3R4)
Proximal 3'UTR (F3R3)
Distal 3'UTR (F4R4)
C
D
E
Normalised Binding (AU)
WT
KO
RKO1
Protein
Protein + Full length 3'UTR
Protein + Proximal 3'UTR
Protein + Distal 3'UTR
F
CstF64
~ 64kDa
G
H
I
Normalised Binding(AU)
Normalise Binding (AU)
ns
J
KO Cell
20 20 20 20 Labelled F3R3(pmol)
0 20 40 80 Unlabelled F3R3(pmol)
HuR
CstF64
INPUT
Protein + Proximal 3'UTR
Unlabelled RNA w.r.t. labelled RNA
0X
2X
4X
8X

◀ **Fig. 3 Arginylation regulated differential binding of HuR and CstF64 to *Hsp70.3* 3′UTR. a** 3′UTR of *Hsp70.3* and its fragments used for in vitro transcription. F3R4: Full length 3′UTR; F3R3: Proximal 3′UTR fragment; and F4R4: Distal 3′UTR fragment. **b–e** Panel **b** represent Western blot for HuR in input and streptavidin retained fractions of WT, KO, and RKO1 MEF extracts incubated with biotinylated RNA fragments of *Hsp70.3* 3′UTR ("Protein + RNA") or with only streptavidin beads without RNA ("Protein"). MEF extracts were prepared post 20 min HS and 2 h recovery. **c–e** represent quantification of streptavidin retained HuR normalized to inputs. (p values are from unpaired t-test, error bar ± SEM, $n = 2$) **f–i** Western blot and graphs represent amount of CstF64 present in same samples represented in **b**. Amount of streptavidin retained CstF64 was normalized to inputs. (p values are from unpaired t-test, error bar ± SEM, $n = 2$) **j** Western blot and graph represent amount of HuR and CstF64 in input and streptavidin retained fractions of KO MEF extracts incubated with 20 pmol biotinylated Proximal 3′UTR (F3R3) fragment of *Hsp70.3* 3′UTR in presence of increasing concentrations (0, 20, 40, 80 pmol) of unlabeled F3R3 RNA. Normalization was done with respect to input samples. (p values are from unpaired t-test, error bar ± SEM, $n = 2$). ns nonsignificant, $^{**}p < 0.05$, $^{***}p < 0.005$.

level could be due to its poly-ubiquitination mediated degradation.

HuR is arginylated at position D15

Mutagenesis of the probable sites of arginylation (E6, D7, E11, D12, C13, D15, and D16) close to N-terminus of mouse HuR were attempted (Fig. S9). Except D7, all other sites were successfully mutated with alanine (A). His-tagged mutant proteins were purified upon over expression in HEK 293T cells, and screened for loss of arginylation by probing with N-term-Arg ab. The loss of arginylation was observed only in the case of D15A mutant (Figs. 6a, S10A, B). To quantify the loss, the ratio of arginylated HuR (R-HuR)/HuR signals were analyzed. While all the mutants showed R-HuR/HuR ratio similar to WT HuR (HuR–His), only in the case of HuR(D15A)–His, the ratio was close to zero (Fig. 6a, S10C, D). HuR(D15A) was stable post-HS compared to faster degrading HuR–His confirmed arginylation dependent degradation of HuR (Fig. 6b).

Arginylation of HuR is a pre-requisite factor for its phosphorylation, in turn regulating its RNA binding activity and APA of *Hsp70.3* pre-mRNA

HuR was arginylated as well as phosphorylated upon HS. As both the modifications apparently inhibited HuR RNA binding, their relationship and sequence required clarification. HuR-His was overexpressed in HEK-293T cells, in presence and absence of BML277 [35–37]. HuR-His was pulled-down, resolved in 1D and 2D-PAGE, and probed with N-term Arg ab (Fig. 6c, d). While BML277 didn't affect HuR arginylation (Fig. 6c), the phosphorylated (acidic) as well as unphosphorylated (basic) spots of HuR-His were detected by N-term Arg ab (Fig. 6d). Thus, upon HS, arginylation preceded phosphorylation of HuR by Chk2. Intriguingly, much of the phospho-HuR spot in the pI range of 3–4 disappeared in case of HuR(D15A)–His (Fig. 6e). Appearance of two new spots at the mid pI range of ~6–7 in HuR(D15A)-His, may indicate a basic shift of the phosphor-HuR spot, due to loss of certain phosphorylations. The spot at the basic end of the blot for HuR (D15A)–His, showed an expected small shift towards lesser pI due to loss of arginylation. HuR amounts were equal in both the samples as observed by 1D Western blot. These results validated arginylation of HuR is a precondition for its phosphorylation.

Further validation was drawn by binding exogenously expressed HuR–His and HuR(D15A)–His from heat-stressed HEK 293T cells with *Hsp70.3* 3′UTR. While HuR–His couldn't interact, HuR(D15A) interacted with the full length 3′UTR fragment (Fig. 6f). Finally, to test if arginylation of HuR does affect APA of *Hsp70.3*, HuR (D15A)–His and HuR–His were over expressed in WT MEFs, and 3′UTR lengths of *Hsp70.3* were analyzed. HuR (D15A)–His expressing cells had a significant fraction of *Hsp70.3* transcripts with long 3′UTR, as compared to untransfected (UT) control and HuR-His expressing cells (Fig. 6g). The phenotype was very similar to that observed in *Ate1* KO cells upon HS. These data confirmed that, arginylation promotes APA of *Hsp70.3* transcripts by facilitating phosphorylation of HuR, which inhibits its recruitment at the 3′UTR of *Hsp70.3*.

Discussion

Apart from its role in normal physiology, involvement of HSP70 in conditions like ischemia, neurodegeneration and cancer, makes it a major therapeutic target [58–62]. Consequently, it is vital to comprehend the regulation of *Hsp70* gene expression; yet the regulation of *Hsp70* expression at post-transcriptional levels is inadequately explored. Earlier we have shown that, loss of arginylation reduces cell viability and destabilizes *Hsp70.3* transcripts [27, 28]. Current study showed arginylation regulates stress-dependent APA of *Hsp70.3*. Previously it was reported that, *Hsp70.3* undergoes APA mediated shortening of 3′UTR, which increases its protein expression [48]. Current study suggested that, APA has a role in stability of the *Hsp70.3* transcripts; as short 3′UTR containing transcripts remained stable, while the long 3′UTR containing transcripts degraded faster (Fig. 1h, i).

HuR, a key regulator of RNA stability, regulates the stability of various stress-related AU rich element (ARE) containing mRNAs, such as c-fos, sirtuin1, urokinase plasminogen activator and its receptor, MAP kinase

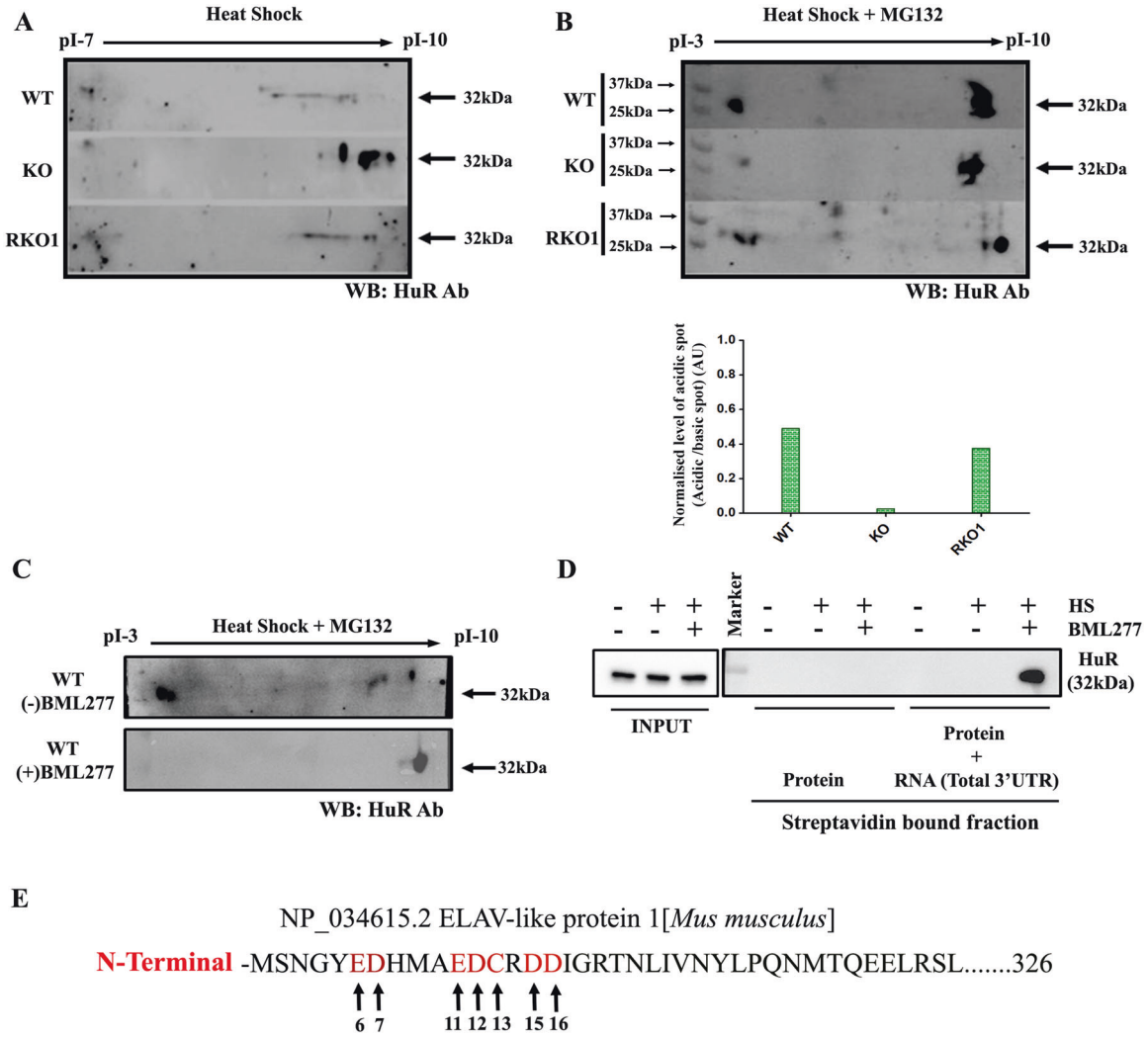

Fig. 4 Arginylation regulates CHK2 dependent phosphorylation of HuR which alters its binding to *Hsp70.3* 3'UTR. a Western blot of heat stressed (20 min HS and 2 h recovery) WT, KO and RKO1 MEF total lysates for HuR after resolving by 2D-PAGE in a linear pI range of 7–10. **b**. Same as **a**, however, cells were treated with MG132 during HS and recovery and proteins were resolved by 2D-PAGE in a linear pI range of 3–10. The bar diagram shows normalized level of the acidic spots of HuR in WT, KO, and RKO1 cells estimated by taking the ratio of HuR signal at the acidic end (~pH 3–4)/HuR signal at the basic end (~pH 9–10). **c** Western blot of heat-stressed (20 min HS and 2 h recovery) and MG132 treated WT MEF total lysates for HuR after resolving by 2D-PAGE in a linear pI range of 3–10. HS was given in presence or absence of CHK2 inhibitor BML277. **d** Western blot for HuR in input and streptavidin retained fractions of WT MEF extracts incubated with biotinylated full length (F3R4) *Hsp70.3* 3′UTR RNA. WT MEF extracts were prepared post 20 min HS and 2 h recovery in presence of MG132 and presence or absence of BML277. **e** N-terminal sequence of *Mus musculus* HuR protein showing aspartic acid (D), glutamic acid (E), and cysteine (C) residues which can act as arginylation sites.

phosphatase 1, p21, etc. Though the protective role of HuR is mostly confined to mature mRNAs, during and after transport to the cytoplasm [54, 56, 63–70], HuR binds to its own pre-mRNA to promote APA [51]. HS dependent modulation of its activity, stability, and localization suggested [50, 71, 72], HuR could be a potential factor regulating arginylation dependent *Hsp70.3* APA.

HuR undergoes HS induced degradation at the early stage of HS response [50]. Stabilization and accumulation of HuR in *Ate1* KO MEFs showed degradation of HuR is ATE1-dependent (Fig. 2b–d). Moreover, enhanced high molecular weight modifications, similar to poly-ubiquitination of HuR, was observed in WT MEFs post HS. Many N-terminally arginylated proteins undergo ubiquitination mediated degradation [1, 2, 10]. However, HuR has never been reported to be an ATE1 target. The current data showed, HuR is arginylated at D15 and the modification is stress-inducible (Figs. 5a, b, 6a). While the mutagenesis of D, E, and C residues near N-terminus identified D15 as the site of arginylation, not all the D, E, and C were mutated. Thus, other sites of arginylation may exist on HuR which could be affected

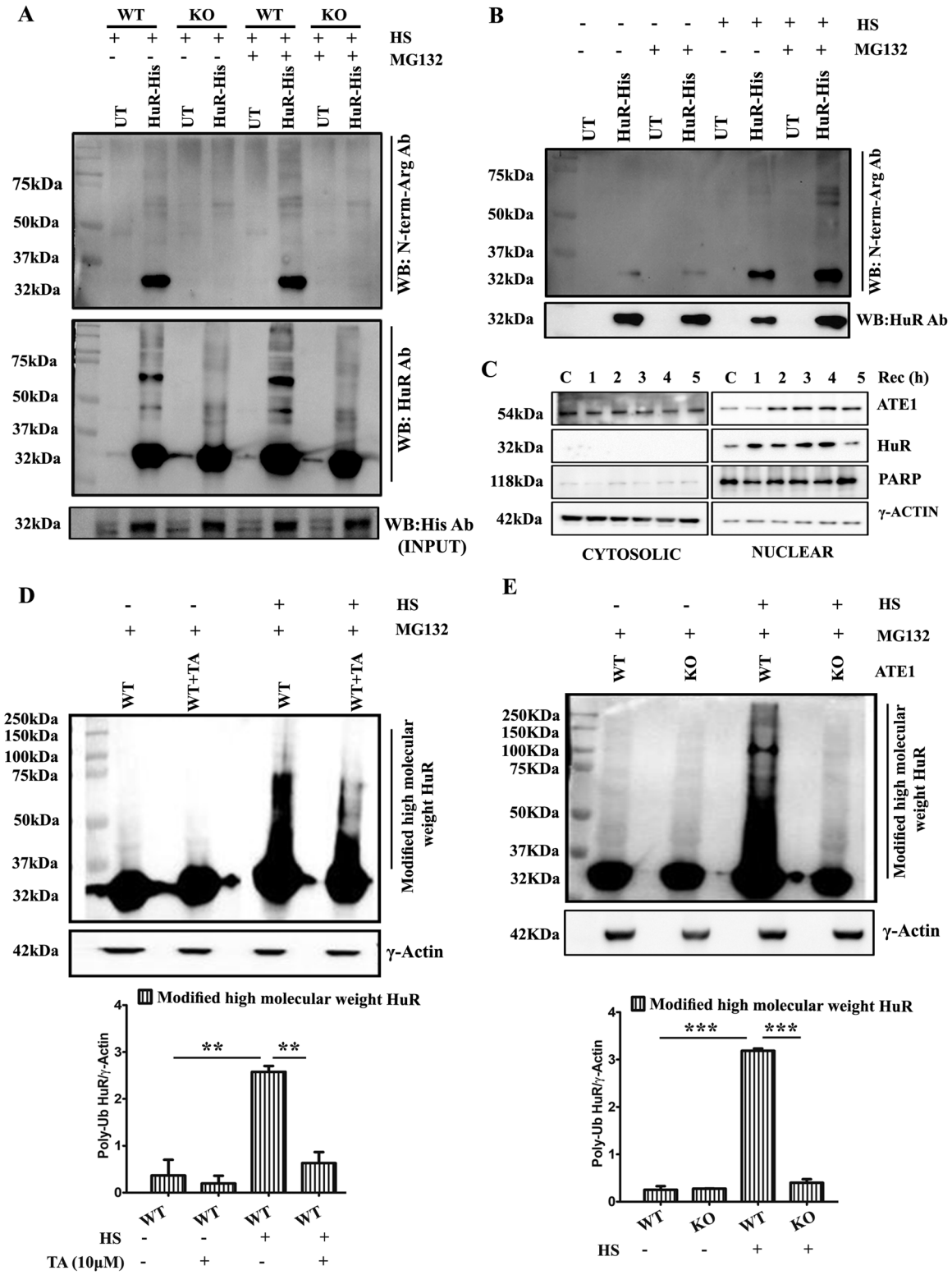

by the mutation of D15. Arginylation deficient HuR mutant HuR(D15A) was stable after HS, demonstrating HuR undergoes arginylation dependent degradation during HS response.

While it was easy to hypothesize that, depletion of HuR upon HS is responsible for the APA of *Hsp70.3*, arginylation concurrently exhibited a greater role in HuR protein than just affecting its stability. Thus, APA of *Hsp70.3* upon

◀ **Fig. 5 HuR acts as a direct target of arginylation and undergoes high molecular weight modification upon HS. a** Western blot for arginylated HuR in MG132 treated heat stressed (20 min HS and 2 h recovery) WT and KO cells transfected with HuR-His followed by Ni-NTA pull down and probing with N-term-Arg Ab. Total content of exogenously expressed pulled HuR was checked by probing with HuR Ab. Inputs were probed with 6× His Ab to check transfection efficiency. Weak signals observed in the similar range of HuR in untransfected cells (UT) with 6× His Ab are due to nonspecific interactions. **b** Western blot for arginylated HuR in control and heat-stressed (20 min HS and 2 h recovery) WT cells transfected with HuR-His followed by Ni-NTA pull down in presence or absence of MG132 and probed with N-term-Arg Ab. Total content of exogenously expressed pulled HuR was checked by probing with HuR Ab. **c** Western blot for ATE1 in cytosolic and nuclear fractions of WT cells at different time points of recovery (1–5 h) post-HS of 20 min. PARP and γ-actin were used as nuclear and cytosolic markers respectively. **d** Western blot represent levels of modified high molecular weight HuR (similar to poly-ubiquitination) in MG132-treated control and heat-stressed (20 min HS and 2 h recovery) WT MEFs in absence and presence of ATE1 inhibitor tannic acid (TA). Graph represent quantifications of high molecular weight forms of HuR normalized with respect to γ-actin. (*p* values are from unpaired *t*-test, error bar ± SEM, $n = 2$). **e** Western blot represent levels of modified high molecular weight HuR (similar to poly-ubiquitination) in MG132-treated control and heat-stressed (20 min HS and 2 h recovery) WT and KO MEFs. Graph represent quantifications of high molecular weight forms of HuR normalized with respect to γ-actin. (*p* values are from unpaired *t*-test, error bar ± SEM, $n = 2$). $^{**}p < 0.05$, $^{***}p < 0.005$.

HS are regulated not by the level of HuR protein, but by the arginylation dependent alteration in RNA binding activity of HuR (Fig. 3b, f). Presence of arginylation on HuR inhibited its binding to *Hsp70.3* 3′UTR, allowing recruitment of CstF64 to proximal PAS, and hence utilization of the proximal PAS. HuR from *Ate1* KO cells bound competitively to proximal PAS, allowing CstF64 to bind distal PAS generating an unstable transcript of *Hsp70.3* with long 3′UTR (Figs. 1e, 3j). Thus, HuR acted at the level of pre-mRNA, and regulated APA of *Hsp70.3* in the nucleus upon HS. Even though the process ultimately stabilized the *Hsp70.3* transcripts, the direct role of HuR in this occasion is to promote APA.

Previous study showed, phosphorylation of HuR by Chk2 during IR stress inhibited its RNA binding activity globally [55]. Current study showed Chk2-mediated HuR phosphorylation is arginylation dependent. Although the detailed cascade of events causing Chk2 mediated phosphorylation of HuR in HS remains to be delineated, results from the current study suggested that arginylation precedes phosphorylation. While inhibition of phosphorylation by Chk2 did not affect arginylation (Fig. 6c, d) loss of arginylation in HuR(D15A) inhibited phosphorylation (Fig. 6e). Comparison of predicted secondary structure of native HuR (1–189 HuR) and truncated HuR with arginylation at the position D15 (R15-189 HuR), showed a change of structure in the loop region harboring the residue S88 which is phosphorylated by Chk2 (Fig. S11). Thus it is possible that, arginylation leads to structural changes in HuR, which might be important for its phosphorylation. Hence, arginylation acted as a pre-requisite for another PTM (like phosphorylation), which in turn regulates the overall activity of its target protein. This was bolstered by the observation that HuR(D15A) from HEK cells (which was deficient of arginylation and phosphorylation), could bind to 3′UTR of *Hsp70.3* and inhibit APA of *Hsp70.3* (Fig. 6f, g).

Though it was suggested that HuR has a protective role on *Hsp70* mature mRNA [49], the present study reports for the first time that HuR regulates stability of *Hsp70.3* transcripts at its pre-mRNA level by its APA. APA is a well-known phenomenon regulating the stability of various transcripts at pre-mRNA stage [47, 73]. APA being a nuclear event and the observed nuclear localization of ATE1 along with HuR at the early stage of HS response support this hypothesis (Fig. 5c).

Our study also endorses the importance of HuR protein level in unstressed and heat-stressed cells. During over-expression of HuR in MEFs, it was observed, higher level of HuR were detrimental for the cells, even in the unstressed condition. This observation suggested a delicate balance of HuR protein level is normally maintained in the cells; and arginylation dependent proteostasis of HuR helps to maintain that balance during HS (Fig. 2g).

Although the reason for enhanced stability of *Hsp70.3* transcripts with short 3′UTR remains to be elucidated, miRNAs could potential be a factor. Earlier reports indicate loss of miR378* binding site at the 3′ UTR of *Hsp70.3* by APA-mediated UTR shortening improves polysome loading [48, 49]. Search of multiple miRNA databases predicted a number of other potential miRNAs, which can bind to the 3′ UTR of mouse *Hsp70.3*, either at the proximal or distal UTR regions (Table S3). Out of the predicted miRNAs, miR-711, miR-215, miR-223, and miR-34a are reported to bind or regulate *Hsp70* expression [48, 74–78]. Intriguingly binding sites for miR-711, miR-215, and miR-223, all are located between the proximal and distal PAS and are lost due to APA. Thus, APA-mediated modulation of miRNA binding can promote Hsp70.3 transcript stability. Exclusion of AU-rich elements (AREs), or GU-rich elements (GREs), or their flanking sequences due to APA, can also increase stability of transcripts [44, 73, 76, 77, 79, 80]. Such sites do exist between the proximal and distal PAS of *Hsp70.3* UTR (Fig. S12). Further studies can elucidate which of these mechanisms are responsible for stabilization of *HSP70.3* transcripts. It will also be important to investigate if arginylation enhances APA of other HS induced transcripts like *Hsp70.1* and *Hsp40*, which were also stabilized upon HS [27, 28].

To conclude, the current study reports HuR as a new target of arginylation, which regulates pre-mRNA

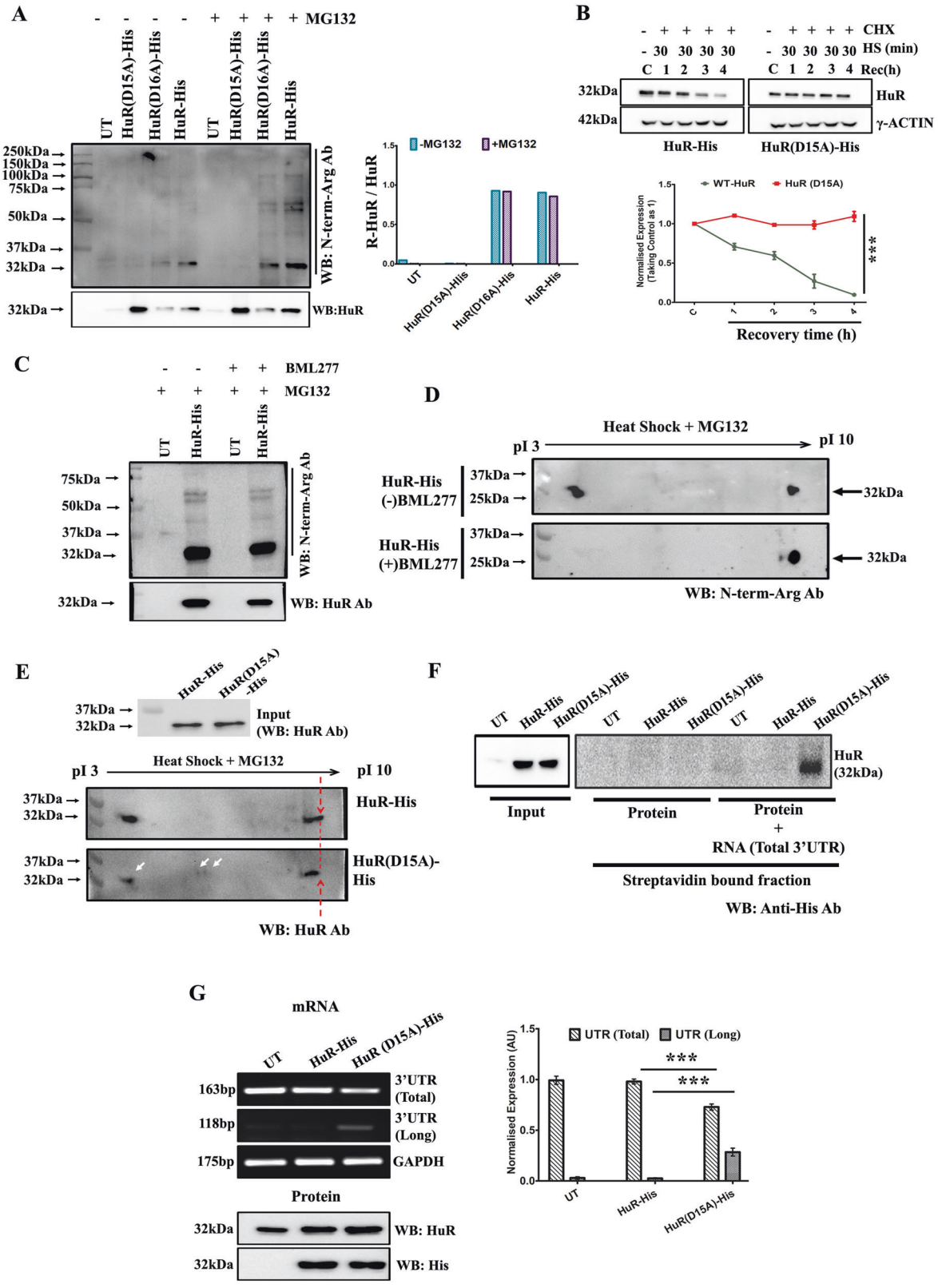

metabolism during HS response. Arginylation coupled phosphorylation of HuR, inhibits its binding to Hsp70.3 pre-mRNA, promoting its APA, which generates stable *Hsp70.3* transcripts with short 3′UTR. At the same time arginylation mediated degradation of HuR helps to maintain its cellular homeostasis, in turn promoting cell viability.

◀ **Fig. 6 Arginylation of HuR at position D15 acts as a pre-requisite factor for its phosphorylation which in turn regulates its RNA binding activity and APA of *Hsp70.3*. a** Western blot for arginylated HuR in MG132-treated heat-stressed (20 min HS and 2 h recovery) HEK293T cells transfected with HuR mutants [HuR(D15A)-His and HuR(D16A)-His] or wild type HuR (HuR–His) followed by Ni-NTA pull down and probing with N-term-Arg Ab. UT untransfected. Total content of exogenously expressed pulled HuR was checked by probing with HuR Ab. Bar diagram represent levels of arginylated HuR normalized to total HuR in the pulled down samples. **b** Western blot and graph represent HuR level in heat-stressed (20 min HS and 4 h recovery) HEK cells transfected with HuR(D15A)-His and HuR-His at different time points of recovery (0–4 h) in presence of cycloheximide (CHX). Samples were normalized with respect to γ-actin. (p values are from one-way ANOVA, error bar ± SEM, $n = 2$) **c** Western blot for arginylated HuR in MG132 +/− BML277-treated heat-stressed (20 min HS and 2 h recovery) HEK293T cells untransfected (UT) or transfected with HuR–His followed by Ni-NTA pull down and probing with N-term-Arg Ab. Total content of exogenously expressed pulled HuR was checked by probing with HuR Ab. **d** Western blot of arginylated HuR from total extracts of heat-stressed (20 min HS and 2 h recovery) HEK293T cells transfected with HuR–His followed by Ni-NTA pull down and resolving by 2D-PAGE in a linear pI range of 3–10. HS was given in presence of MG132 +/− BML277. WB: N-term-Arg Ab. **e** Western blots of Ni-NTA pulled down HuR after resoling by 1D and 2D PAGE (pI range of 3–10). HEK293T cells transfected with HuR–His and HuR(D15A)–His were subjected to heat stress (20 min HS and 2 h recovery) in presence of MG132 followed by Ni-NTA pull down and Western blotting of HuR. WB: HuR Ab. White arrows indicate changes in the phosphorylated spot of HuR and appearance of new spots possibly due to basic shifts caused by loss of certain phosphorylation. **f** Western blot for HuR present in input and streptavidin retained fraction of heat-stressed (20 min HS and 2 h recovery) untransfected (UT), HuR–His and HuR(D15A)–His transfected HEK cell extracts incubated with biotinylated full length (F3R4) 3′UTR of *Hsp70.3*. WB: 6× His Ab. **g** Normalized level of total *Hsp70.3* transcript and transcripts having long 3′UTR with respect to GAPDH in untransfected (UT), HuR–His, and HuR(D15A)-His transfected WT MEFs following HS of 30 min with 2 h recovery. (p values are from unpaired t-test, error bar ± SEM, $n = 3$) $^{***}p < 0.005$.

Acknowledgements We thank Dr Anna Kashina (University of Pennsylvania, USA) for the WT and KO MEFs, ATE1 antibody. pMSCV-PIG was kindly provided by Dr David Bartel (MIT, USA). We thank Dr. A. N. Jha and Ms Sapna M. Borah, TU for their help with structure analysis; Dr. Gaurangi Maitra for careful editing of the text. SS is supported by SERB-India (EEQ/2016/000772 and EMR/2016/004001). KD is supported by scholarship from SERB-India (EEQ/2016/000772). We thank funding agencies for their support to MBBT, TU (UGC-SAP, DST FIST, DBT Strengthening, DBT-Hub, and DBT-BIF) and Department of Biotechnology, NIT, Durgapur (DST-FIST).

Compliance with ethical standards

Conflict of interest The authors declare that they have no conflict of interest.

Publisher's note Springer Nature remains neutral with regard to jurisdictional claims in published maps and institutional affiliations.

References

1. Bachmair A, Finley D, Varshavsky A. In vivo half-life of a protein is a function of its amino-terminal residue. Science. 1986;234:179–86.
2. Ferber S, Ciechanover A. Role of arginine-tRNA in protein degradation by the ubiquitin pathway. Nature. 1987;326:808.
3. Kaji H, Kaji A. Protein modification by arginylation. Chem Biol. 2011;18:6–7.
4. Kaji H. Amino-terminal arginylation of chromosomal proteins by arginyl-tRNA. Biochemistry. 1976;15:5121–5.
5. Wong CC, Xu T, Rai R, Bailey AO, Yates 3rdJR, Wolf YI, et al. Global analysis of posttranslational protein arginylation. PLoS Biol. 2007;5:e258.
6. Wang J, Han X, Wong CC, Cheng H, Aslanian A, Xu T, et al. Arginyltransferase ATE1 catalyzes midchain arginylation of proteins at side chain carboxylates in vivo. Chem Biol. 2014;21:331–7.
7. Eriste E, Norberg Å, Nepomuceno D, Kuei C, Kamme F, Tran D-T, et al. A novel form of neurotensin post-translationally modified by arginylation. J Biol Chem. 2005;280:35089–97.
8. Wang J, Pejaver VR, Dann GP, Wolf MY, Kellis M, Huang Y, et al. Target site specificity and in vivo complexity of the mammalian arginylome. Sci Rep. 2018;8:16177.
9. Wang J, Han X, Leu NA, Sterling S, Kurosaka S, Fina M, et al. Protein arginylation targets alpha synuclein, facilitates normal brain health, and prevents neurodegeneration. Sci Rep. 2017;7:1–14.
10. Elias S, Ciechanover A. Post-translational addition of an arginine moiety to acidic NH2 termini of proteins is required for their recognition by ubiquitin-protein ligase. J Biol Chem. 1990;265:15511–7.
11. Karakozova M, Kozak M, Wong CC, Bailey AO, Yates JR, Mogilner A, et al. Arginylation of ß-actin regulates actin cytoskeleton and cell motility. Science. 2006;313:192–6.
12. Saha S, Mundia MM, Zhang F, Demers RW, Korobova F, Svitkina T, et al. Arginylation regulates intracellular actin polymer level by modulating actin properties and binding of capping and severing proteins. Mol Biol Cell. 2010;21:1350–61.
13. Zhang F, Patel DM, Colavita K, Rodionova I, Buckley B, Scott DA, et al. Arginylation regulates purine nucleotide biosynthesis by enhancing the activity of phosphoribosyl pyrophosphate synthase. Nat Commun. 2015;6:7517.
14. Piatkov KI, Brower CS, Varshavsky A. The N-end rule pathway counteracts cell death by destroying proapoptotic protein fragments. Proc Natl Acad Sci. 2012;109:E1839–47.
15. Rai R, Zhang F, Colavita K, Leu NA, Kurosaka S, Kumar A, et al. Arginyltransferase suppresses cell tumorigenic potential and inversely correlates with metastases in human cancers. Oncogene. 2016;35:4058.
16. Singh A, Borah AK, Deka K, Gogoi AP, Verma K, Barah P, et al. Arginylation regulates adipogenesis by regulating expression of PPARγ at transcript and protein level. Biochim Biophys Acta. 2019;1864:596–607.
17. Davydov IV, Varshavsky AJJoBC. RGS4 is arginylated and degraded by the N-end rule pathway in vitro. J Biol Chem. 2000;275:22931–41.
18. Cha-Molstad H, Sung KS, Hwang J, Kim KA, Yu JE, Yoo YD, et al. Amino-terminal arginylation targets endoplasmic reticulum chaperone BiP for autophagy through p62 binding. Nat Cell Biol. 2015;17:917.
19. Decca MB, Carpio MA, Bosc C, Galiano MR, Job D, Andrieux A, et al. Post-translational arginylation of calreticulin: a new isospecies of calreticulin component of stress granules. J Biol Chem. 2007;282:8237–45.
20. Lee MJ, Tasaki T, Moroi K, An JY, Kimura S, Davydov IV, et al. RGS4 and RGS5 are in vivo substrates of the N-end rule pathway. Proc Natl Acad Sci. 2005;102:15030–5.
21. White MD, Klecker M, Hopkinson RJ, Weits DA, Mueller C, Naumann C, et al. Plant cysteine oxidases are dioxygenases that directly enable arginyl transferase-catalysed arginylation of N-end rule targets. Nat Commun. 2017;8:14690.

22. Carpio MA, Decca MB, Sambrooks CL, Durand ES, Montich GG, Hallak ME. Calreticulin-dimerization induced by post-translational arginylation is critical for stress granules scaffolding. Int J Biochem Cell Biol. 2013;45:1223–35.
23. Zhang F, Saha S, Kashina A. Arginylation-dependent regulation of a proteolytic product of talin is essential for cell–cell adhesion. J Cell Biol. 2012;197:819–36.
24. Saha S, Kashina A. Posttranslational arginylation as a global biological regulator. Dev Biol. 2011;358:1–8.
25. Hu R-G, Sheng J, Qi X, Xu Z, Takahashi TT, Varshavsky A. The N-end rule pathway as a nitric oxide sensor controlling the levels of multiple regulators. Nature. 2005;437:981.
26. Lamon KD, Kaji H. Arginyl-tRNA transferase activity as a maker of cellular aging in peripheral rat tissues. Exp Gerontol. 1980;15:53–64.
27. Deka K, Singh A, Chakraborty S, Mukhopadhyay R, Saha S. Protein arginylation regulates cellular stress response by stabilizing HSP70 and HSP40 transcripts. Cell Death Discov. 2016;2:16074.
28. Deka K, Saha S. Arginylation: a new regulator of mRNA stability and heat stress response. Cell Death Dis. 2017;8:e2604.
29. Banerji S, Berg L, Morimoto RI. Transcription and post-transcriptional regulation of avian HSP70 gene expression. J Biol Chem. 1986;261:15740–5.
30. Morimoto RI, Kroeger P, Cotto J. The transcriptional regulation of heat shock genes: a plethora of heat shock factors and regulatory conditions. In: Stress-inducible cellular responses. (Eds. Feige U, Yahara I, Morimoto RI, Polla BS) New York: Springer; 1996. p. 139–63.
31. Morimoto RI. Cells in stress: transcriptional activation of heat shock genes. Science. 1993;259:1409–1409.
32. Theodorakis NG, Morimoto RI. Posttranscriptional regulation of hsp70 expression in human cells: effects of heat shock, inhibition of protein synthesis, and adenovirus infection on translation and mRNA stability. Mol Cell Biol. 1987;7:4357–68.
33. Kwon YT, Kashina AS, Davydov IV, Hu R-G, An JY, Seo JW, et al. An essential role of N-terminal arginylation in cardiovascular development. Science. 2002;297:96–99.
34. Mayr C, Bartel DP. Widespread shortening of 3′ UTRs by alternative cleavage and polyadenylation activates oncogenes in cancer cells. Cell. 2009;138:673–84.
35. Arienti KL, Brunmark A, Axe FU, McClure K, Lee A, Blevitt J, et al. Checkpoint kinase inhibitors: SAR and radioprotective properties of a series of 2-arylbenzimidazoles. J Med. Chem. 2005;48:1873–85.
36. Dai B, Zhao XF, Mazan-Mamczarz K, Hagner P, Corl S, Bahassi EM, et al. Functional and molecular interactions between ERK and CHK2 in diffuse large B-cell lymphoma. Nat Commun. 2011;2:1–9.
37. Thakuri PS, Gupta M, Singh S, Joshi R, Glasgow E, Lekan A, et al. Phytochemicals inhibit migration of triple negative breast cancer cells by targeting kinase signaling. BMC Cancer. 2020;20:1–14.
38. Roy A, Kucukural A, Zhang Y. I-TASSER: a unified platform for automated protein structure and function prediction. Nat Protoc. 2010;5:725.
39. Yang J, Zhang Y. I-TASSER server: new development for protein structure and function predictions. Nucleic Acids Res. 2015;43:W174–81.
40. Zhang Y. I-TASSER server for protein 3D structure prediction. BMC Bioinform. 2008;9:40.
41. Hinman M, Lou H. Diverse molecular functions of Hu proteins. Cell Mol Life Sci. 2008;65:3168.
42. Pettersen EF, Goddard TD, Huang CC, Couch GS, Greenblatt DM, Meng EC, et al. UCSF Chimera—a visualization system for exploratory research and analysis. J Comput Chem. 2004;25:1605–12.
43. de Lorenzo L, Sorenson R, Bailey-Serres J, Hunt AG. Non-canonical alternative polyadenylation contributes to gene regulation in response to hypoxia. Plant Cell. 2017;29:1262–77.
44. Graham RR, Kyogoku C, Sigurdsson S, Vlasova IA, Davies LR, Baechler EC, et al. Three functional variants of IFN regulatory factor 5 (IRF5) define risk and protective haplotypes for human lupus. Proc Natl Acad Sci. 2007;104:6758–63.
45. Hollerer I, Curk T, Haase B, Benes V, Hauer C, Neu-Yilik G, et al. The differential expression of alternatively polyadenylated transcripts is a common stress-induced response mechanism that modulates mammalian mRNA expression in a quantitative and qualitative fashion. RNA. 2016;22:1441–53.
46. Liu Y, Hu W, Murakawa Y, Yin J, Wang G, Landthaler M, et al. Cold-induced RNA-binding proteins regulate circadian gene expression by controlling alternative polyadenylation. Sci Rep. 2013;3:2054.
47. Zheng D, Wang R, Ding Q, Wang T, Xie B, Wei L, et al. Cellular stress alters 3′ UTR landscape through alternative polyadenylation and isoform-specific degradation. Nat Commun. 2018;9:2268.
48. Tranter M, Helsley RN, Paulding WR, McGuinness M, Brokamp C, Haar L, et al. Coordinated post-transcriptional regulation of Hsp70. 3 gene expression by microRNA and alternative polyadenylation. J Biol Chem. 2011;286:29828–37.
49. Kraynik SM, Gabanic A, Anthony SR, Kelley M, Paulding WR, Roessler A, et al. The stress-induced heat shock protein 70.3 expression is regulated by a dual-component mechanism involving alternative polyadenylation and HuR. Biochim Biophys Acta. 2015;1849:688–96.
50. Abdelmohsen K, Srikantan S, Yang X, Lal A, Kim HH, Kuwano Y, et al. Ubiquitin-mediated proteolysis of HuR by heat shock. EMBO J. 2009;28:1271–82.
51. Dai W, Zhang G, Makeyev EV. RNA-binding protein HuR autoregulates its expression by promoting alternative polyadenylation site usage. Nucleic Acids Res. 2011;40:787–800.
52. Dickson AM, Anderson JR, Barnhart MD, Sokoloski KJ, Oko L, Opyrchal M, et al. Dephosphorylation of HuR protein during alphavirus infection is associated with HuR relocalization to the cytoplasm. J Biol Chem. 2012;287:36229–38.
53. Grammatikakis I, Abdelmohsen K, Gorospe M. Posttranslational control of HuR function. Wiley Interdiscip Rev. 2017;8:e1372.
54. Abdelmohsen K, Pullmann JrR, Lal A, Kim HH, Galban S, Yang X, et al. Phosphorylation of HuR by Chk2 regulates SIRT1 expression. Mol Cell. 2007;25:543–57.
55. Masuda K, Abdelmohsen K, Kim MM, Srikantan S, Lee EK, Tominaga K, et al. Global dissociation of HuR–mRNA complexes promotes cell survival after ionizing radiation. EMBO J. 2011;30:1040–53.
56. Fan XC, STEITZ JA. Overexpression of HuR, a nuclear–cytoplasmic shuttling protein, increases the in vivo stability of ARE-containing mRNAs. EMBO J. 1998;17:3448–60.
57. Saha S, Wang J, Buckley B, Wang Q, Lilly B, Chernov M, et al. Small molecule inhibitors of arginyltransferase regulate arginylation-dependent protein degradation, cell motility, and angiogenesis. Biochem Pharmacol. 2012;83:866–73.
58. Kaur P, Hurwitz MD, Krishnan S, Asea A. Combined hyperthermia and radiotherapy for the treatment of cancer. Cancers. 2011;3:3799–823.
59. Murphy ME. The HSP70 family and cancer. Carcinogenesis. 2013;34:1181–8.
60. Tranter M, Ren X, Forde T, Wilhide ME, Chen J, Sartor MA, et al. NF-κB driven cardioprotective gene programs; Hsp70. 3 and cardioprotection after late ischemic preconditioning. J Mol Cell Cardiol. 2010;49:664–72.
61. Turturici G, Sconzo G, Geraci F. Hsp70 and its molecular role in nervous system diseases. Biochem Res Int. 2011;2011.

62. Wu G, Osada M, Guo Z, Fomenkov A, Begum S, Zhao M, et al. ΔNp63α up-regulates the Hsp70 gene in human cancer. Cancer Res. 2005;65:758–66.
63. Peng SSY, Chen CYA, Xu N, Shyu AB. RNA stabilization by the AU-rich element binding protein, HuR, an ELAV protein. EMBO J. 1998;17:3461–70.
64. Brennan C, Steitz J. HuR and mRNA stability. Cell Mol life Sci. 2001;58:266–77.
65. Güttinger S, Mühlhäusser P, Koller-Eichhorn R, Brennecke J, Kutay U. Transportin2 functions as importin and mediates nuclear import of HuR. Proc Natl Acad Sci. 2004;101:2918–23.
66. REBANE A, AAB A, STEITZ JA. Transportins 1 and 2 are redundant nuclear import factors for hnRNP A1 and HuR. RNA. 2004;10:590–9.
67. Gallouzi I-E, Steitz JA. Delineation of mRNA export pathways by the use of cell-permeable peptides. Science. 2001;294:1895–901.
68. Wang Z, Kiledjian M. The poly (A)-binding protein and an mRNA stability protein jointly regulate an endoribonuclease activity. Mol Cell Biol. 2000;20:6334–41.
69. Tran H, Maurer F, Nagamine Y. Stabilization of urokinase and urokinase receptor mRNAs by HuR is linked to its cytoplasmic accumulation induced by activated mitogen-activated protein kinase-activated protein kinase 2. Mol Cell Biol. 2003;23:7177–88.
70. Wang W, Furneaux H, Cheng H, Caldwell MC, Hutter D, Liu Y, et al. HuR regulates p21 mRNA stabilization by UV light. Mol Cell Biol. 2000;20:760–9.
71. Gallouzi I-E, Brennan CM, Stenberg MG, Swanson MS, Eversole A, Maizels N, et al. HuR binding to cytoplasmic mRNA is perturbed by heat shock. Proc Natl Acad Sci. 2000;97:3073–8.
72. GALLOUZI I-E, BRENNAN CM, STEITZ JA. Protein ligands mediate the CRM1-dependent export of HuR in response to heat shock. RNA. 2001;7:1348–61.
73. Tian B, Manley JL. Alternative polyadenylation of mRNA precursors. Nat Rev Mol Cell Biol. 2017;18:18.
74. Fesler A, Xu X, Zheng X, Li X, Jiang J, Russo JJ, et al. Identification of miR-215 mediated targets/pathways via translational immunoprecipitation expression analysis (TrIP-chip). Oncotarget. 2015;6:24463.
75. Sabirzhanov B, Stoica B, Zhao Z, Loane D, Wu J, Dorsey S, et al. miR-711 upregulation induces neuronal cell death after traumatic brain injury. Cell Death Differ. 2016;23:654.
76. Place RF, Noonan EJ. Non-coding RNAs turn up the heat: an emerging layer of novel regulators in the mammalian heat shock response. Cell Stress Chaperones. 2014;19:159–72.
77. Tang Q, Yuan Q, Li H, Wang W, Xie G, Zhu K, et al. miR-223/Hsp70/JNK/JUN/miR-223 feedback loop modulates the chemoresistance of osteosarcoma to cisplatin. Biochem Biophys Res Commun. 2018;497:827–34.
78. Shehata RH, Abdelmoneim SS, Osman OA, Hasanain AF, Osama A, Abdelmoneim SS, et al. Deregulation of miR-34a and its chaperon Hsp70 in hepatitis C virus-induced liver cirrhosis and hepatocellular carcinoma patients. Asia Pac J Cancer Prev. 2017;18:2395.
79. Moraes KC, Wilusz CJ, Wilusz J. CUG-BP binds to RNA substrates and recruits PARN deadenylase. RNA. 2006;12:1084–91.
80. Ueno S, Sagata N. Requirement for both EDEN and AUUUA motifs in translational arrest of Mos mRNA upon fertilization of Xenopus eggs. Dev Biol. 2002;250:156–67.